Selective Silica Removal in Geothermal Brines: Implications for Applications for Geothermal Power Plant Operation and Brine Mining

Laura Spitzmüller[a,1], Valentin Goldberg[a], Sebastian Held[a], Jens C. Grimmer[a], Daniel Winter[b], Milena Genovese[b], Joachim Koschikowski[b], Thomas Kohl[a]

[a] Institute of Applied Geosciences, Division Geothermal Energy and Reservoir Technology, Karlsruhe Institute of Technology, Adenauerring 20b, 76131 Karlsruhe, Germany

[b] Fraunhofer Institute for Solar Energy Systems ISE, Heidenhofstraße 2, 79110 Freiburg, Germany

Abstract

Raw material extraction from geothermal brines often comprises concentrating and cooling steps, which increases the risk of silica scaling formation. However, existing silica removal strategies do not consider the impact on raw material extraction. In this study, the applicability and element-selectivity of three silica removal techniques (seed-induced, lime and caustic precipitation) were tested in batch experiments using synthetic and natural brine samples. Increasing the pH-value to 10.5 and the Ca/Si ratio > 1.25 was found to mitigate silica scaling effectively via formation of calcium-silicate-hydrate phases. The developed silica removal process does not affect the raw materials and is therefore suitable for brine mining purposes.

Keywords: silica scaling mitigation, lithium, brine mining, C-S-H phases, mineral extraction, selective silica removal

1. Introduction

Geothermal brines may attain high silica concentrations during fluid-rock interaction at high temperatures (Fournier and Rowe, 1966; Henley, 1983; Iler, 1979). The brines are thus assumed to be in equilibrium with silica under reservoir conditions. Cooling and brine concentrating processes involved in geothermal power plant operation cause the saturation index (SI) of silica to increase to SI ≥ 0 and hence precipitation may commence. In flash-steam geothermal power plants with operational temperatures ≥ 200 °C brine concentration occurs due to the steam-phase separation. The resulting increase of the silica concentration in the residual brine may lead to scaling problems, depending on initial silica concentration and the fraction of steam-phase separation (e.g. Setiawan et al., 2019). In binary geothermal power plants, commonly operating at temperatures of 120 °C < T < 200 °C, cooling-induced silica oversaturation of the brine may occur in the reinjection pipeline.

Recently, geothermal brines moved into focus as a new source for several raw materials such as Li (Bourcier et al., 2005). However, the concentration of the raw materials in brines is relatively low compared to conventional deposits (Kesler et al., 2012; Schmidt, 2017). Therefore, concentration of the brines as a pre-treatment process may be required to increase the effectiveness of raw material extraction (Ryu et al., 2016). Thus brines with relatively low ion-concentrations (Tassi et al., 2010) may become economically viable resources. However, power plant operations as well as raw material extraction processes increase the risk of silica scaling significantly.

Silica removal prior to cooling or enrichment of the brine can therefore be crucial for both geothermal power plant operation and brine mining. For economic, environmental and sustainability reasons silica

---

[1] Corresponding author.
E-Mail address: laura.spitzmueller@kit.edu

precipitates should not contain environmentally harmful elements or substances as they must be either disposed or re-used as a product. Furthermore, the silica precipitates should not contain elements of economic interest, as they are the target of a later stage mineral extraction process. This concerns especially for Li, Zn, Cs, Rb, and trace elements like B, Ag, and Au (Bourcier et al., 2005; Maimoni, 1982; Neupane and Wendt, 2017). Moreover, highly pure silica and silicates are valuable raw materials themselves (Johnston et al., 2019, Lee et al., 2018, Mathieux et al., 2017). There are various approaches to extract silica from geothermal brines (e.g. Bourcier et al., 2001, 2006; Finster et al., 2015; Lin et al., 2002, 2003; Mroczek et al., 2015), which are limited to low saline brines. For highly saline brines, there is a lack of information about commercial silica extraction.

This study is associated with the German-Chilean BrineMine project[2] funded by the Federal Ministry of Education and Research (BMBF). The project aims to develop a system for sustainable raw material and drinking water production from thermal waters in Chile. The developed methods shall derive alternative mining concepts to the conventional mineral extraction as in the Salars of the Atacama Desert, which are associated with high environmental impact. Therefore, this study consists of two parts: The first part comprises lab experiments with synthetic brines inspired by the composition of the waters in the El Tatio geothermal field in northern Chile. The main focus is to develop a silica removal strategy that does not affect the raw materials, especially the lithium concentrations. In the second part we apply the developed processes on a natural, complex brine from a thermal spring in Baden-Baden (e.g. Stober, 2002), close to the Eastern Main Boundary Fault of the Upper Rhine Graben (Grimmer et al., 2017). The main focus is also on silica removal and conservation of Li concentrations in the brine, whereas a minor focus is on the behavior of trace elements.

2. Materials and Methods

This study aims to develop a selective silica removal strategy to enable raw material extraction from geothermal brines. Therefore, different silica scaling mitigation techniques were tested using synthetic and natural brine samples to identify the most effective silica removal process. A special focus is on their impact on raw materials and trace elements.

2.1 Review of silica scale mitigation techniques

Generally, scaling mitigation techniques are distinguished into inhibition and precipitation methods. The use of synthetic inhibitors for silica scaling mitigation has turned out to be ineffective due to the amorphous structure of the silica scales (Gallup, 2002; Gallup and Barcelon, 2005; Milne et al., 2014; Neofotistou and Demadis, 2004). The most promising inhibition method is the pH adjustment to retard the polymerization and aggregation of silica (Bourcier et al., 2005; Finster et al., 2015; Gallup, 2002, 2011; Kiyota and Uchiyama, 2011; Rothbaum et al., 1979; Sigfusson and Gunnarsson, 2011). In the framework of mineral extraction further cooling or concentration processes are required that may increase the SI≫0 (Gunnarsson and Arnórsson, 2005). In this case, even the pH adjustment will not prevent silica precipitation.

Milne et al. (2014) provide an overview of the state-of-the-art techniques for silica removal. Techniques like electrocoagulation and ion exchange can be excluded in this study due to high investment costs. Table 1 provides an overview of the most promising silica removal techniques. The lime precipitation method is by far the most common method and has shown good applicability in geothermal settings (Table 1). The use of metal salt addition techniques is not desired since the metal ions remain in solution and can affect potential raw material extraction processes and - depending on the used metal - may be a raw or economically interesting material itself and hence the use of metal cations is neither economic nor ecologic reasonable (Milne et al., 2014). The lime, the caustic, and the

---

[2] BrineMine Project: https://www.bmbf-client.de/en/projects/brinemine

seed-induced precipitation processes are considered as most promising, because required materials are widely distributed and easily accessible. For the lime precipitation method (Borrmann and Johnston, 2017; Cairns et al., 2006) and the silica seeding method (Setiawan et al., 2019) analyses of the chemical composition of the precipitates exist, but the behavior of lithium and other raw material were not considered. The analysis of the precipitates with a focus on lithium behavior is therefore emphasized in this study.

Table 1. Overview of the most common silica removal techniques.

Method	Additive	Reference
Seed-induced precipitation	Silica seeds	Setiawan et al. (2019), Sugita et al. (1999; 2003)
Lime precipitation	Ca(OH)$_2$	Badruk and Matsunaga (2001), Borrmann et al. (2009), Borrmann and Johnston (2017), Kato et al. (2003), Putera et al. (2018), Rothbaum and Anderton (1975), Vitolo and Cialdella (1994)
Caustic precipitation	NaOH	Gallup et al. (2003)
Metal salt addition	Zn	Zeng et al. (2007)
	Al	Sugita et al. (1999), Yokoyama et al. (1989)
	Fe	Gallup et al. (2003), Renew and Hansen (2017)
	Mg	Lin et al. (2003), Morita et al. (2017)
	Cu	Gallup et al. (2003)

2.2 Brine synthesis

A synthetic, trace-element-free brine was used to study the effectiveness of various silica removal techniques and their impact on the lithium concentration in solution. A complex natural brine was used to validate the applicability of a selected silica removal process with a special focus on the behavior of trace elements.

2.2.1 Synthetic brine

Silica removal experiments were conducted with a synthetic brine for comparability and reproducibility. The composition of the brine was synthesized based on the chemical composition of the El Tatio geothermal waters, Northern Chile (Chapter 1, Table 2, Ellis and Mahon, 1977, Giggenbach, 1978, Tassi et al., 2010). Hereby, only the main and redox-insensitive anions and cations were used for the synthesis of the synthetic brine. Experimental conditions as well as silica concentration were adapted to simulate the cooled thermal fluid (cooled down from ~210°C) of a geothermal power plant considered for reinjection with a temperature of 70 °C, leading to a supersaturation regarding silica.

For synthesis, both a salt solution and a silica solution were prepared separately to avoid unintended immediate precipitation during dissolution of the components. The salt solution contains NaCl (Merck EMSURE, assay 99.5 %), KCl (Merck EMSURE, assay 99.5 %), Na$_2$SO$_4$ (Merck EMSURE, assay 99 %), LiOH (Merck EMSURE, assay 98 %), and CaCl$_2$ (VWR Chemicals, assay 94 %), dissolved in double-distilled water. The pH was adjusted to pH 6.7 using HCl (Merck Supelco, 37 %). The silica solution was prepared by mixing double distilled water with silica (Merck, extra pure) and NaOH (Merck EMSURE, assay 99 %) to obtain a solution with pH > 12. For complete dissolution we performed magnetic stirring with c. 500 rpm at 70 °C in an oven for more than 12 hours. Before mixing the solutions, the pH of the silica (+NaOH) solution was adjusted to pH 6.7 using HCl. The quantity of added salts was adjusted to yield the concentrations shown in Table 2 after mixing. HDPE vessels were used during the whole synthesis process to exclude contamination by amorphous silica from glass containers. For each experiment, the synthetic silica solution was freshly prepared to exclude polymerization effects that may occur with time.

2.2.2   Adapted natural brine

For the experiments using a natural thermal fluid, the Baden-Baden brine ("Fettquelle", FQ) was selected due to its public accessibility. The Na-Cl-rich brine contains a TDS of 2.9 g/L (Sanjuan et al., 2016) and 131 mg/L SiO_2 (Table 5). As the SiO_2 concentration deviates from deep geothermal fluids from URG (Sanjuan et al. 2016), the natural brine was modified before the experiments (Table 2). The concentration was increased twice by evaporation. Additionally, the concentration of Li was raised to about 100 mg/L by addition of LiCl (Sigma Aldrich, assay 99 %) and the concentration of Cs was raised to 10 mg/L by addition of CsCl (Merck Suprapur, assay 99.5 %) to be in the range of geothermal fluids of the URG and also enable a detectability in the precipitates. Both elements are of economic value and therefore of particular interest.

Table 2. Chemical composition of the El Tatio well T5 brine (Giggenbach, 1978), the synthetic brine, the Baden-Baden Fettquelle (FQ) thermal spring (Sanjuan et al., 2016) and the adapted natural brine (twice the concentration of the natural FQ brine). For the synthetic brine and the adapted natural brine mean values and standard deviations of ion concentrations are given.

Parameter	Unit	El Tatio T5	Synthetic brine	Baden-Baden FQ	Adapted natural brine
pH	-	6.7	6.7 ± 0.1	7.82	8.0 ± 0.1
Temperature	°C	212	69 ± 1	61	70.2 ± 0.3
TDS	mg/L	11,813	10,725 ± 280.8	2900	n.d.
Li^+	mg/L	32	32 ± 0.15	8.0	95.02 ± 1.53
Na^+	mg/L	3760	3686 ± 162	827	1815 ± 71.05
K^+	mg/L	519	518 ± 2.4	86.7	169.07 ± 6.43
Cs^+	mg/L	13.1	n.a.	0.7	10
Ca^{2+}	mg/L	219	215 ± 10.7	122	174.35 ± 4.32
Mg^{2+}	mg/L	n.d.	n.a.	3.96	7.78 ± 0.17
SiO_2	mg/L	343	343 ± 0.6	131	290.56 ± 3.48
Cl^-	mg/L	6690	6136 ± 280	1480	n.d.
SO_4^{2-}	mg/L	34	34.5 ± 0.7	140	n.d.

n.d. not determined
n.a. not added

2.3 Additives

Four different additives were used for the silica removal experiments (Fig. 1): Silica seeds (Merck, extra pure), $Ca(OH)_2$ (Merck EMSURE, assay 96 %), $CaCl_2$ (VWR Chemicals, assay 94 %), and NaOH (Merck EMSURE, assay 99 %). Silica seeds and $Ca(OH)_2$ proved to be effective for the removal of silica according to literature (Chapter 2.1, Table 1). $CaCl_2$ and NaOH are chosen to identify respective effects of Ca-ions and pH separately. The following experiments were conducted using synthetic brine:

- Addition of silica seeds to the synthetic solution with a 10x higher concentration of the silica seeds to the SiO_2 content in solution. The brine was synthesized without Ca to eliminate a possible impact on the removal mechanism.
- $Ca(OH)_2$ was added with a special focus on the impact of the molar calcium-to-silicon-ratio (Ca/Si ratio). Note that addition of $Ca(OH)_2$ affects the Ca/Si ratio and the pH at the same time.
- To study the sole impact of the pH value, different concentrations and amounts of NaOH were used to adjust the pH. The Ca/Si ratio was set to 2.0 by addition of $CaCl_2$.
- The sole impact of the Ca/Si ratio was studied by adjusting the ratio with different amount of $CaCl_2$. In this case, the pH was fixed at 10.5 by addition of NaOH.

Out of the four additives, the most effective one is chosen to validate the batch experiments using an adapted natural brine.
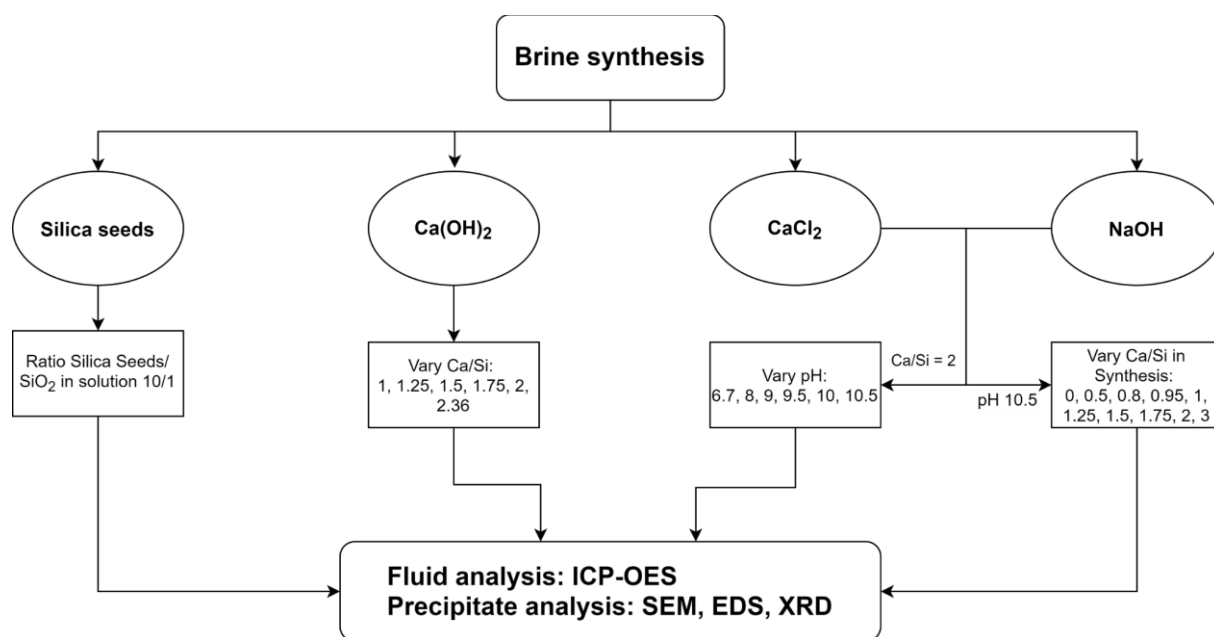

Fig. 1. Experimental scheme from synthesis of a synthetic brine to analysis. The different additives are marked bold. The fluid analysis (ICP-OES results) show a time series of a 120 minutes reaction time interval for each experiment, whereas the precipitate analysis is performed solely for the precipitates after the reaction time interval. Ca/Si is the (initial) molar calcium-to-silicon-ratio.

2.4 Experimental setup

The experimental setup is similar for the experiments using synthetic brine and for the experiments using adapted natural brine. The precipitation experiments were carried out at 70 °C in an oven under magnetic stirring at 500 rpm in 1L-HDPE vessels. About 600 mL of the brines (Chapter 2.2) were used for each experiment. Solution samples were taken before adding the seeding material (Fig. 1) and after the addition selectively in a 120 minutes time interval. The fluid samples were taken according to the following procedure. 1 mL of the solution was filtered through a syringe using a cellulose acetate filter (0.45 µm) to remove solids. By diluting the aliquot 1:100 with double distilled water further reactions were prevented. Temperature and pH of the solution were measured during sampling. After 120 minutes of reaction time, the brine was filtered using a vacuum pump and a 0.45 µm cellulose acetate filter. The precipitates were collected and dried overnight in the oven at 70 °C. The fluid samples were measured focusing on the cations using an ICP-OES (Varian 715-ES). The uncertainty was determined from the deviations of the standard solutions. The analyses of the dried precipitates were performed with XRD (Bruker D8), SEM (Tescan Vega), and EDS (Inca X Act). Additionally, the precipitates of the experiments with natural brine are washed with double distilled water and collected by centrifugation (6000 rpm, 30 minutes). This step is performed to remove potential salt crust layers which may have formed during the drying process. The precipitates are dissolved using a HNO_3-HF-$HClO_4$-acid mixture and measured with an ICAP-RQ Thermo Fischer ICP-MS.

3. Results

3.1 Removal experiments using synthetic brine

23 experiments were carried out following the experimental scheme shown in Table 1. Selected results are presented in this section to emphasize the trend observed in the experiments. Detailed results are listed in Table 4. A special focus is on the silica removal effectiveness and the conservation of the Li concentration.

The results of the precipitation experiments depicting on the SiO₂ and the Li concentration are shown in Fig. 2. These experiments contribute to assess and to compare the methods (Chapter 2). Fig. 2A compares the residual SiO₂ concentrations, while Fig. 2B displays the Li concentration. Addition of Ca(OH)₂ and NaOH caused an effective reduction of the silica concentration while the Li concentration has remained constant. In contrast, the addition of silica seeds as well as the addition of CaCl₂ did not show a significant reduction of the residual SiO₂ concentration. Furthermore, the Li concentration was reduced by 19 % in the silica seeding experiment.
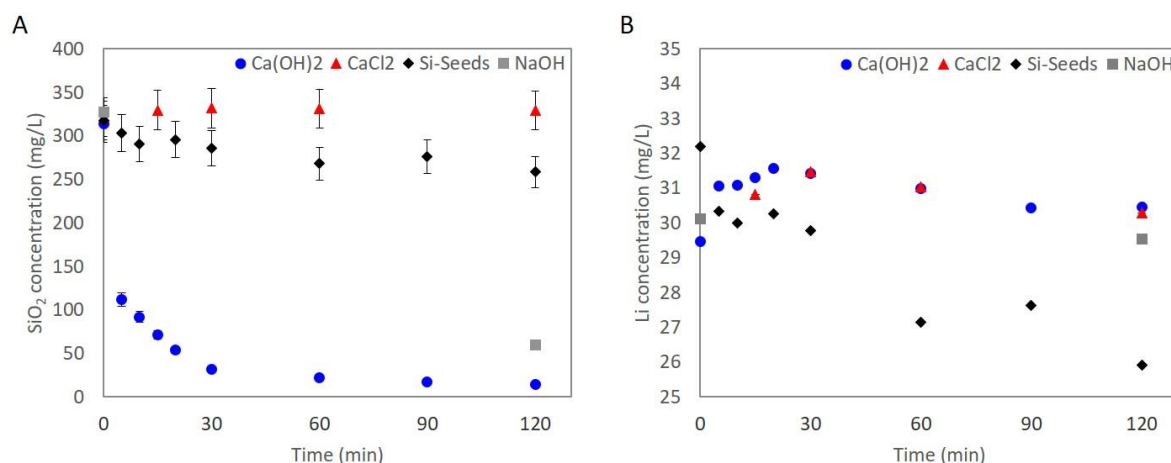

Fig. 2. Comparison of the residual SiO₂ (A) and Li (B) concentration after precipitation experiments with Ca(OH)₂, CaCl₂, silica seeds, and NaOH (Exs. 16, 2, 1, 23, Table 4). For the CaCl₂ and NaOH experiments, not each time step has been sampled. The error bars represent the percentage error of the ICP-OES analysis and are calculated by the deviation from the standard solution. The errors are unique for each experimental trial and each cation.

Fig. 3 shows the usage of Ca(OH)₂ as precipitation agent (Fig. 3A) and the addition of silica seeds (Fig. 3B) in more detail. After the addition of Ca(OH)₂ the pH raised immediately from initial 6.7 to 10.5 ± 0.1. The temperature remained constant at 69 °C. The molar Ca/Si ratio was raised from an initial Ca/Si ratio of 0.95 to 2.36 after the addition of 590 mg Ca(OH)₂ per liter. The SiO₂ concentration was reduced below the saturation concentration of 230 mg/L (reference at 70 °C and pH 6.7, PHREEQC LLNL database) within minutes and maintained constantly below 20 mg/L. Within 120 minutes, about 96 % of the initial silica concentration was removed, whereby 68 % was removed within the first 5 minutes and 94 % within 30 minutes after the addition of Ca(OH)₂. The concentrations of Li, K, and Na were not affected by the addition of the precipitation agent. The Ca concentration was raised due to the addition of Ca(OH)₂, but the theoretical maximum concentration of 539 mg/L Ca, which would comprise the initial plus the added Ca, was not reached. Fig. 3B shows the results of the addition of silica seeds. In contrast to the precipitation experiment with Ca(OH)₂, the SiO₂ concentration could not be reduced below the saturation concentration of 230 mg/L. Furthermore, the Li concentration decreases about 19 % to 25.93 mg/L, the K concentration decreases about 17 % to 444 mg/L and the Na concentration is reduced by 17 % to 3139 mg/L (Table 4). Therefore, the silica seeding method did not prove to be effective in terms of effective and selective silica removal.
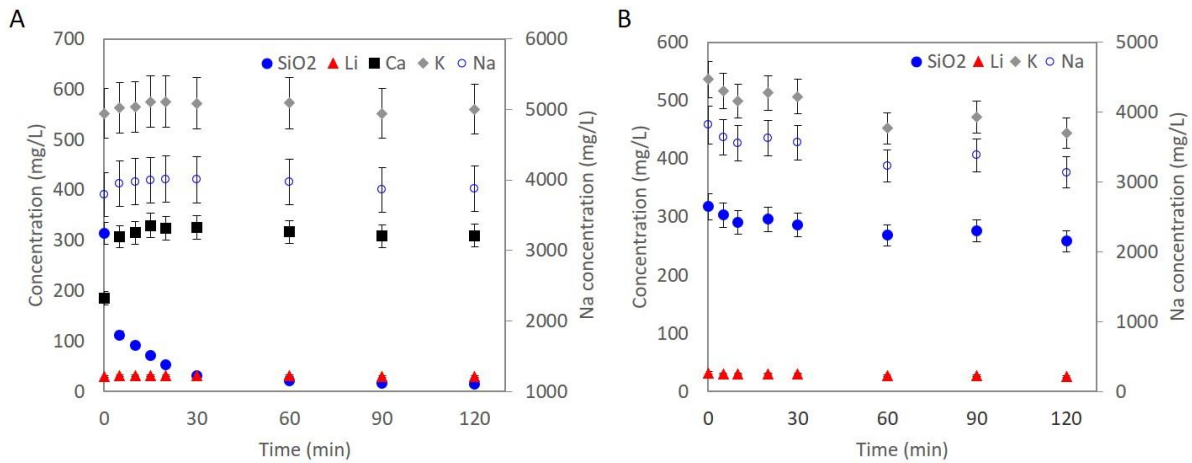
Fig. 3. ICP-OES results of the precipitation experiments with Ca(OH)$_2$ (A) and silica seeds (B) (Exs. 16, 1, Table 4). Samples were taken over a time of 120 minutes after addition of the additive. Note that the Na concentration is shown on the 2nd y-axis. The error bars represent the percentage error of the ICP-OES analysis and are calculated by the deviation from the standard solution. The errors are unique for each experimental trial and each cation.

Fig. 4 shows the SEM images and the EDS spectra of the precipitates from the different experiments (Exs. 1, 16, 23, Table 4). The precipitates from the experiments with Ca(OH)$_2$ and NaOH (Fig. 4A & C) have, according to the EDS spectra, Si and Ca as the main components. In accordance with the XRD analysis patterns, the precipitates can be classified as calcium-silicate-hydrates (C-S-H). The C-S-H phases have porous structures as reported in the literature (Borrmann and Johnston, 2017; Cairns et al., 2006). The EDS spectra for the precipitate resulting from the addition of NaOH (Fig. 4C) possess higher Na, K, and Cl concentrations compared to the EDS spectra of the precipitate adding Ca(OH)$_2$ (Fig. 4A). Furthermore, the precipitates have a more solid morphology than the porous flakes resulting from the Ca(OH)$_2$ treatment. This indicates coverage of the C-S-H with salts. In accordance with the XRD analysis patterns, halite and sylvite are expected. Furthermore, the XRD patterns reveal the presence of calcite in the precipitates resulting from the Ca(OH)$_2$ and the NaOH treatment. Calcite as carbonate can not be analyzed with EDS spectra due to the coverage of the samples with carbon. Furthermore, calcite was not visible in the SEM imaging, which indicates a microcrystalline structure.

The silica seeds (Fig. 4B) could be analyzed with SEM and EDS, but due to the amorphous structure, no XRD analysis could be performed. The silica seeds do not show a difference between the recovered and the initial morphology.
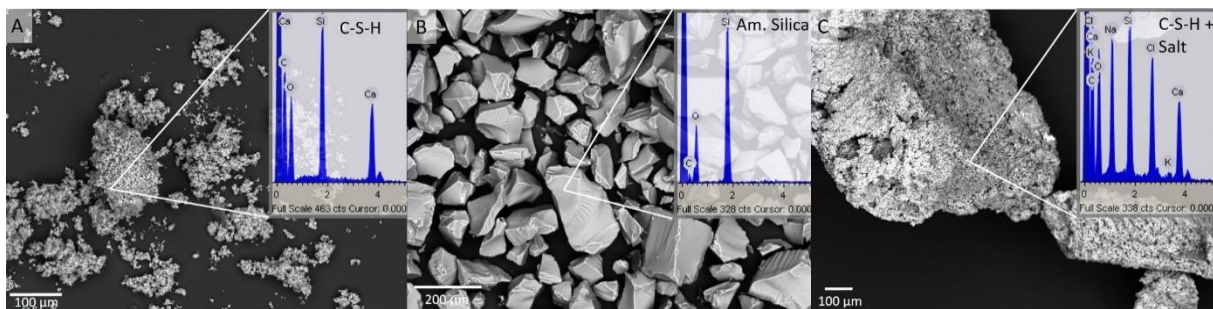

Fig. 4. SEM and EDS spectra of the precipitates. After the Ca(OH)$_2$ (A) and the NaOH (C) treatment, C-S-H is observed as precipitate in form of small, porous flakes, whereas in the silica seeding experiments (B) the output products look similar to silica seed input.

3.2 Process validation using adapted natural brine

The methods developed in this study were tested with synthetic brines in batch experiments to analyze the driving forces behind silica precipitation. The general applicability for complex brines was

examined by further experiments with an adapted natural thermal brine from the Baden-Baden spring (Chapter 2.2). Besides the silica removal, the focus of this experiment series was on the incorporation of trace elements in the precipitates that could not be investigated using a synthetic, trace-element-free fluid. The experiments shall determine a possible impact of trace elements on the removal mechanism and the selectivity of the precipitation mechanism. The previously described batch experiments with $Ca(OH)_2$ as additive have shown the highest removal effectiveness (Fig. 2). Therefore, this method was selected to treat the Baden-Baden brine. For verification, three different but similar samples of the natural brine from FQ were prepared by evaporative concentration. The different samples are denoted as Bad 1, Bad 2, and Bad 3.

Fig. 5 shows the ICP-OES results of the fluid phase of the $Ca(OH)_2$ precipitation experiments. Three similar trials were performed following the experimental setup described in Chapter 2. Detailed results can be found in Table 5. Fig. 5A shows the evolution of the SiO_2 concentration within the 120 minutes reaction time interval in the fluid phase. For all samples tested, the decrease of the SiO_2 concentration occurs immediately after the addition of the $Ca(OH)_2$. Li (Fig. 5B), as well as Na (Fig. 5D), remain unaffected, whereas Mg is reduced below the detection limit during the experiment (Fig. 5C). Sr and Rb show a slight decrease (Fig. 5C). The precipitates consist in the majority of calcite and C-S-H phases as measured in the XRD. SEM and EDS identify the presence of Ca and Si (Fig. 6). Due to the low initial concentration of Mg, it was not detected in the EDS or SEM. Clear identification of the incorporation process of trace elements and hence the purity of the product can be derived from the analysis of precipitates using ICP-MS. The results are shown in Fig. 7. Mn and Sr show the highest incorporation in the precipitates with concentrations of 170-600 ppm and 450-600 ppm respectively. However, the incorporation of trace elements accounts only for a lesser amount (<0.25 %, Table 6).
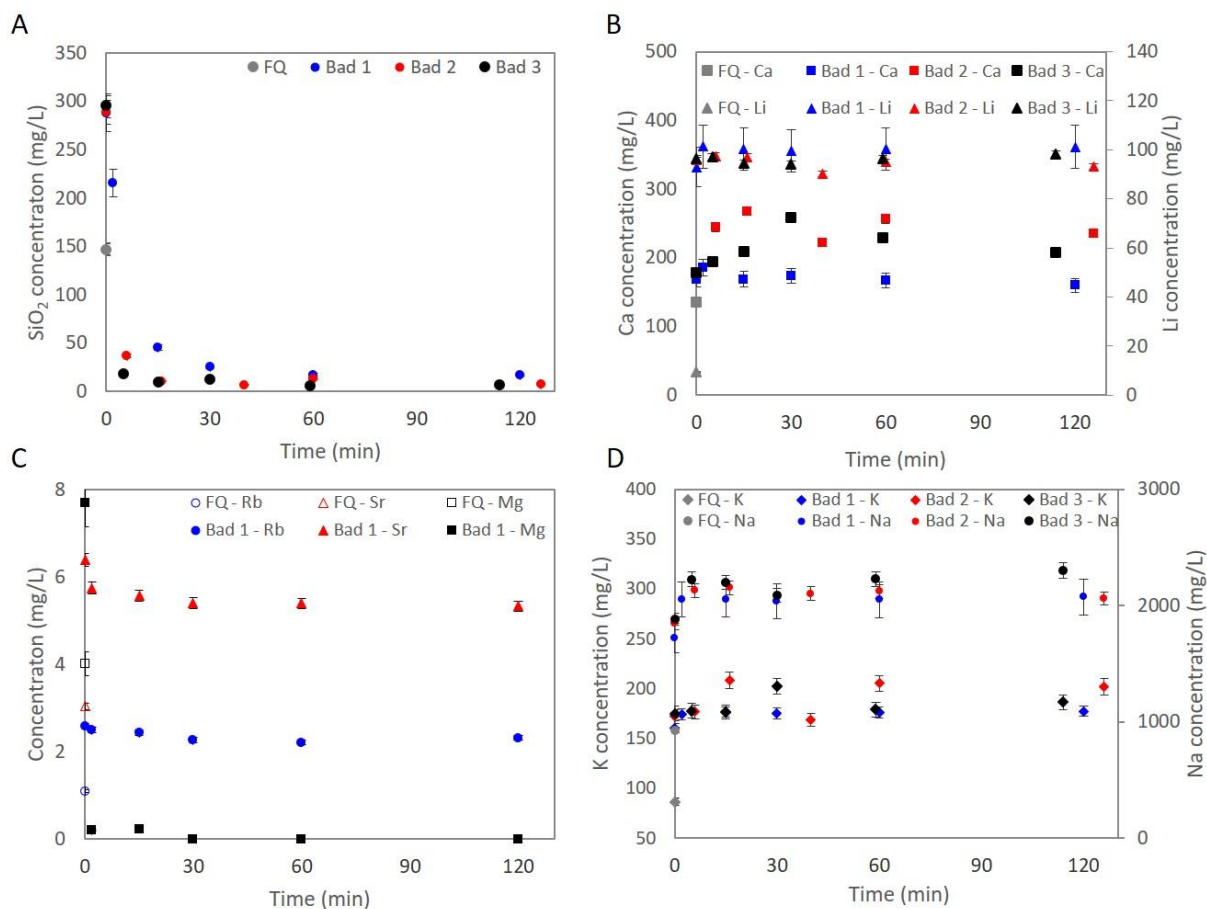

Fig. 5. ICP-OES results of the precipitation experiments with the thermal water from Baden-Baden. FQ shows the initial contents before concentrating the fluid. The precipitation was achieved by addition of $Ca(OH)_2$ and NaOH to raise the pH over

10.5. Note the different y_2-axis scaling at B and D. C only shows the results of Bad 1. Mg was below detection limit after 30 minutes (C).
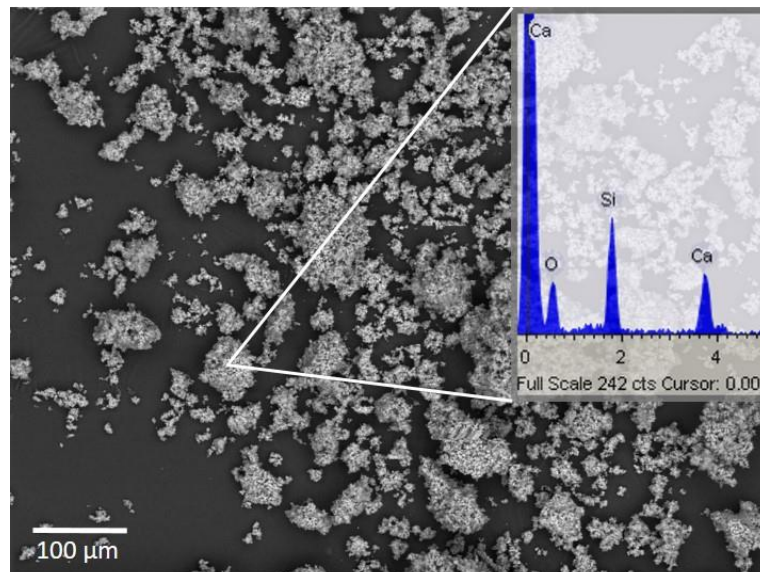

Fig. 6. SEM and EDS spectra of the Baden-Baden precipitate after treatment with Ca(OH)$_2$. The small, porous flakes show a C-S-H composition and have a similar morphology as the precipitates shown in Fig. 4.
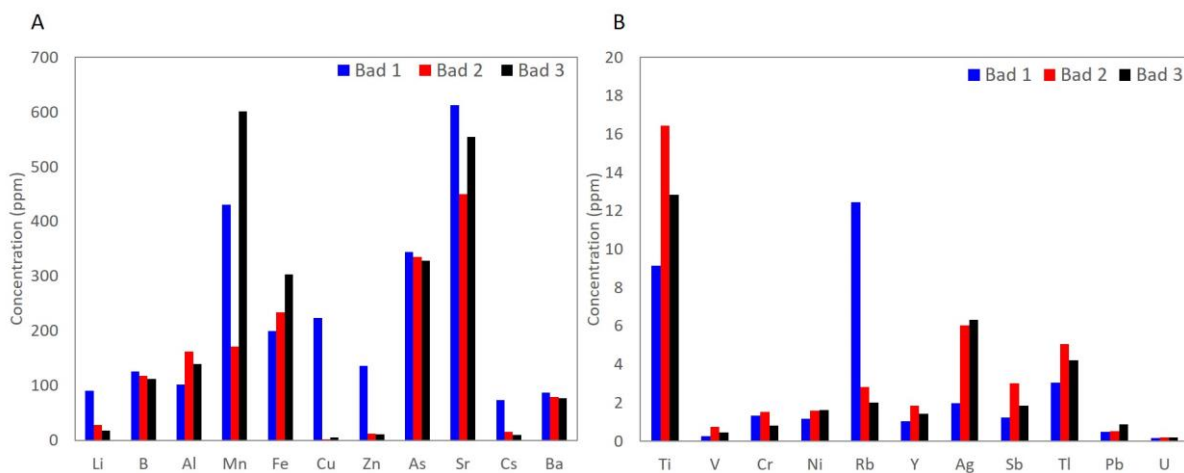

Fig. 7. Trace element content of the precipitates Bad 1, Bad 2 and Bad 3 analyzed with ICP-MS. Mn and Sr show the highest incorporation in the precipitates with concentrations of 170-600 ppm (Mn) and 450-600 ppm (Sr). However, the total amount of incorporated trace elements is summed up to less than 0.25 %.

4. Discussion

This study aims to develop a selective, element-specific silica removal process that does not affect the raw material concentration in brines and is therefore suitable for brine mining purposes. Three different existing silica removal techniques were tested focusing on their removal effectiveness and their impact on raw materials.

4.1 Silica seeding

As indicated in the ICP-OES results (Fig. 3), the EDS and SEM analysis (Fig. *4*B), the silica seeds did not show significant incorporation of other elements despite silica itself. The reduction of the SiO$_2$ concentration is achieved by interaction between silicic acid (H$_4$SiO$_4$) and the silica seed surface leading to precipitation (Bremere et al., 2000; Sugita et al., 2000). The ability of amorphous silica seeds to induce the nucleation and polymerization of silicic acid is already well known and is applied in some geothermal power plants (Bremere et al., 2000; Setiawan et al., 2019; Sugita et al., 1999). The major

disadvantage of the method can be observed in the experiments: The removal effectiveness of the method is depending on the difference between the initial silica concentration and the saturation concentration (Bremere et al., 2000; Sugita et al., 1999). Below the saturation concentration, no further removal of SiO_2 occurs. Since brine concentrating would cause again supersaturation of silica, it is not sufficient to reduce the concentration to saturation. For a concentration of raw materials in the brine by a factor of 5 to 10 the silica content must be reduced to 1/5 to 1/10 of the saturation concentration to avoid unwanted precipitation.

4.2 C-S-H formation

The precipitation mechanism for the experiments with $Ca(OH)_2$, NaOH and $CaCl_2$ + NaOH can be identified as the formation of C-S-H phases (Fig. 4A & C). Two factors are crucial for the SiO_2 removal via C-S-H-phases: alkaline pH-values and the availability of Ca. The interaction of both factors favors the formation of C-S-H phases. The addition of $Ca(OH)_2$ yields SiO_2 concentrations much below similar experiments with NaOH (Fig. 2). Although both experiments were performed at the same pH of 10.5, the Ca/Si ratio differs: for NaOH it was the initial Ca/Si ratio of 0.95 (Table 2), for the trial with $Ca(OH)_2$ addition the Ca/Si was raised to 2.36. Vice versa, the increase of the Ca/Si ratio with $CaCl_2$ did not show similar results to the $Ca(OH)_2$ experiments, even though the experiments with $CaCl_2$ were performed at an identical Ca/Si ratio of 2.36. Unlike $Ca(OH)_2$, the addition of $CaCl_2$ did not increase the pH. As a conclusion, it can be stated that for an effective removal of Si via C-S-H phases formation, an alkaline pH value as well as a sufficiently high Ca/Si ratio need to be reached.

To examine the impact of the Ca/Si ratio on the removal effectiveness, experiments with different Ca/Si ratios were analyzed at a constant pH value. The Ca/Si ratio was set by the addition of $CaCl_2$ without affecting the pH (Fig. 1). The pH value of each experiment was fixed to 10.5 using NaOH. The initial SiO_2 concentrations were 340 mg/L. Fig. 8 shows the residual SiO_2 and the residual Ca concentration after 60 to 120 minutes of reaction time for different molar Ca/Si ratios. According to Greenberg (1954), not all Ca in solution reacts with the SiO_2, therefore molar Ca/Si ratios > 1 would improve the effectiveness of the precipitation methods significantly. This behavior is confirmed by the lab experiments (Fig. 8). Minimum residual SiO_2 concentrations are reached at a Ca/Si ratio > 1.25. At higher ratios, no further significant decrease is observed. For applications in raw material extraction and power plant operations, the residual Ca concentration also needs to be minimized to avoid e.g. calcite scaling. Therefore, the optimal method yields both, minimal residual SiO_2 and Ca concentrations. As the residual Ca concentrations increase with higher initial molar Ca/Si ratios and the residual SiO_2 concentration does not further significantly decrease, Ca/Si ratios between 1.25 and 1.5 are favorable.
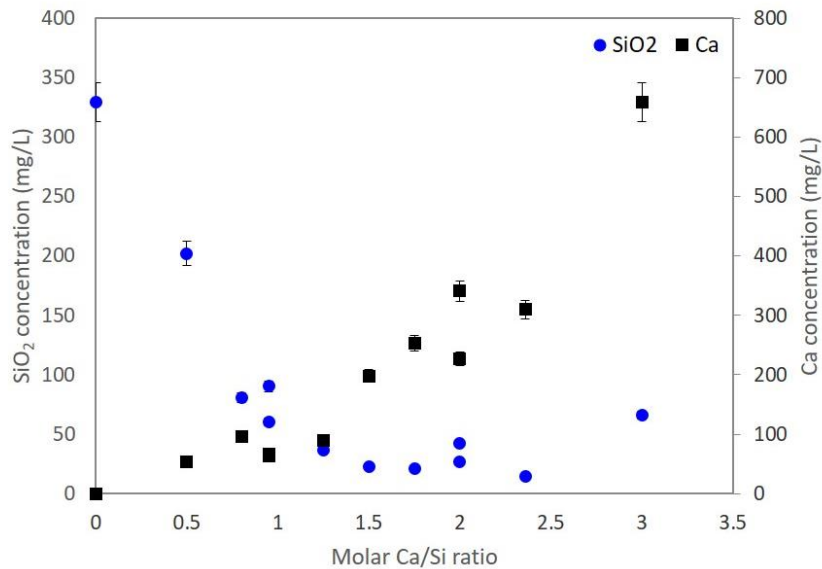
Fig. 8. Impact of the molar Ca/Si ratio on the removal of SiO_2 and the residual Ca concentration. The pH is set to 10.5 by addition of NaOH (Exs. 7-16, 22, 23, Table 4).

Fig. 9 illustrates the impact of the pH on the residual SiO_2 concentration. The initial SiO_2 concentration was 340 mg/L (Table 2, Table 4) for all experiments, which results in an initial Ca/Si ratio of 0.95. Fig. 9 clearly states that the removal of SiO_2 is independent of the precipitation method used. The decisive factor is the increase of the pH to values > 10 for a more effective reduction of the SiO_2 concentration underneath the silica saturation. Explications can be provided by the silica species distribution. At pH > 10 the $H_3SiO_4^-$ species is exceeding the H_4SiO_4 species by far (Alexander et al., 1954; Eikenberg, 1990; Iler, 1979). The $H_3SiO_4^-$ species favors the adsorption of divalent ions on the surface (Greenberg, 1956). The adsorbed Ca^{2+} ion enhances the interparticle bridging (Iler, 1975, 1979; Maraghechi et al., 2016) and consequently the formation of C-S-H precipitates. Phases, precipitation because of oversaturation

Young Matsuyama2000 -> effects of ph on precipitation of quasi crystalline csh phases in aquoues solutions
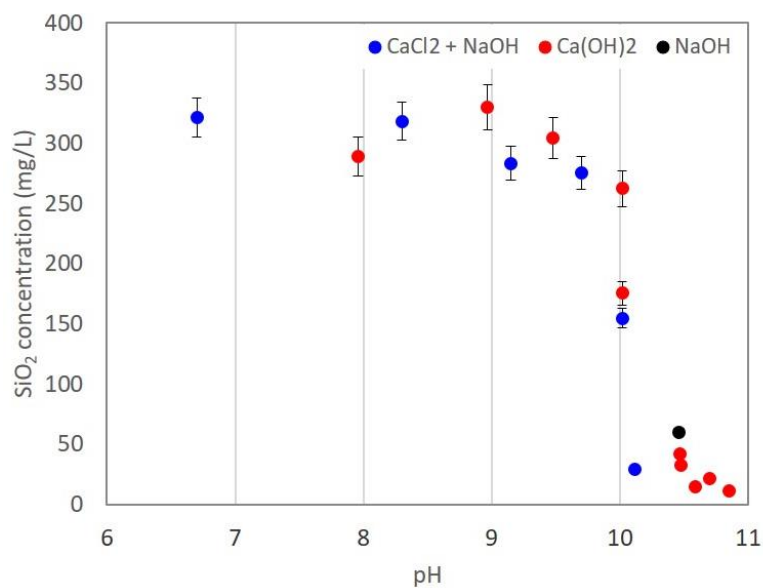

Fig. 9. Impact of the pH on the reduction of the SiO_2 concentration. Three different methods to raise the pH are shown (Exs. 3-7, 16-21, 23, Table 4). They all prove to be effective at pH > 10, unaffected by the additive.

For the understanding of the incorporation process in the natural brine experiments, the element enrichment in the precipitates is calculated with respect to the concentration in the fluid (Fig. 10). Monovalent elements (Li, Rb, Cs) are depleted in the precipitate in comparison to the fluid, while divalent or higher valent elements are enriched in the precipitates. Hence, the incorporation of the trace elements seems to be dependent on the valence of the ions. However, the incorporation of trace elements is summed up to below 0.25 % (Fig. 7). The only element which is clearly affected by the precipitation process is Mg. Mg could not be detected in ICP-MS analysis, because the measurement setup was focused on the trace element detection. However, the decrease in the fluid samples (Fig. 5) hints on the incorporation of Mg in the precipitation process resulting in the simultaneous formation of M-S-H and C-S-H phases.
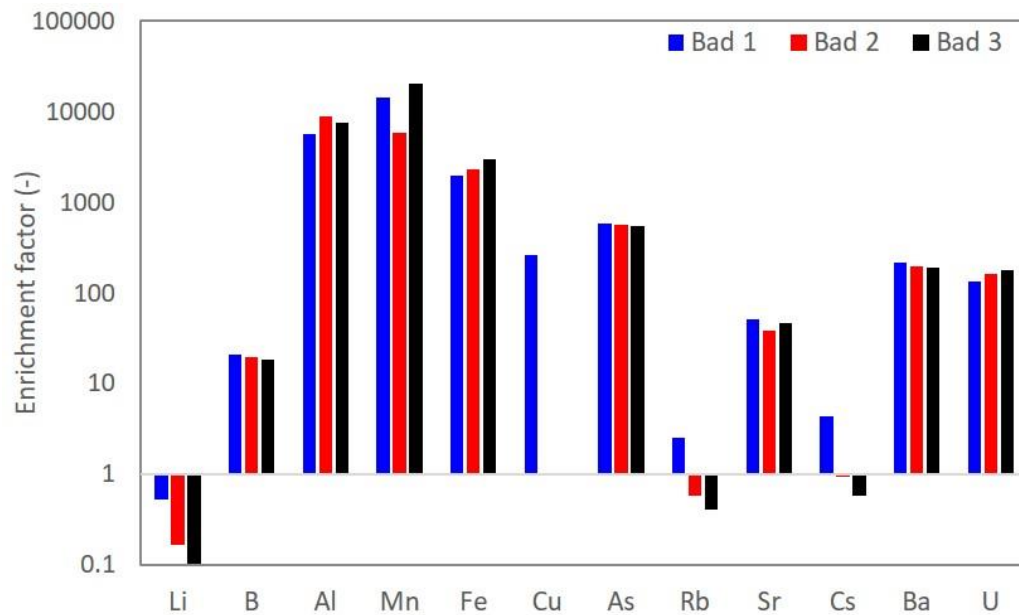
Fig. 10. Enrichment factors of the trace elements. The enrichment factors are calculated by dividing the percentage of the element in the solid phase by the percentage in the fluid. Enrichment factors greater than 1 indicate an accumulation of the element in the solid phase, whereas factors minor 1 indicate an accumulation in the fluid phase.

Fig. 11 compares the removal effectiveness of our experimental setting with comparable results found in literature. To ensure comparability with the laboratory experiments, only experiments with similar SiO_2 and TDS concentrations and a comparable amount of additive used are taken into account (Table 3). Precipitation methods with $Ca(OH)_2$, Zn, and Al as additives appear to be most effective. The silica seeding method in this study is less effective than the comparative methods described in the literature. The deviation can be explained by the experimental setup: The experiments in the literature were performed with a higher initial SiO_2 concentration and a lower temperature (Setiawan et al., 2019). This leads to higher removal effectiveness, although the method is not able to reduce the SiO_2 concentration below saturation. As indicated in literature, silica removal processes using $Ca(OH)_2$ and NaOH are highly effective. In comparison with the literature data, our batch experiments with $Ca(OH)_2$ show even a higher removal effectiveness. Furthermore, our results indicated that also the addition of NaOH yields similar SiO_2 reduction rates, if the solution contains sufficient high Ca/Si ratios.

Fig. 11. Comparison of the removed SiO_2 in the experiments with results found in literature for different precipitation methods. Silica Seeds: Setiawan et al. (2019), Ex. 1 (T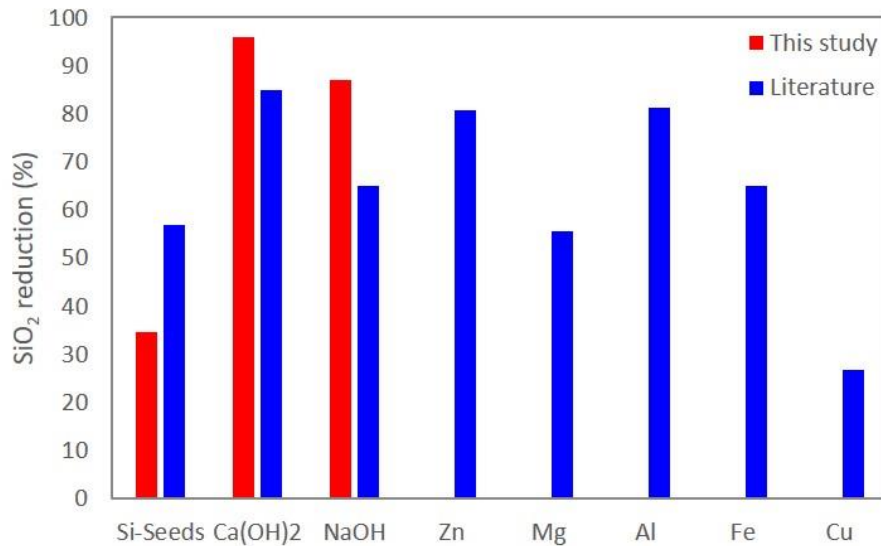able 4), Ca(OH)$_2$: Badruk and Matsunaga (2001), Ex. 16 (Table 4), NaOH: Gallup et al. (2003), Ex. 23 (Table 4), Zn: Zeng et al. (2007), Mg: Lin et al. (2003), Al: Yokoyama et al. (2002), Fe: Renew and Hansen (2017), Cu: Gallup et al. (2003).

Table 3: Comparison of the SiO_2 removal effectiveness of different precipitation methods from literature data (mg/L, unless otherwise noted).

Method	SiO_2 initial	SiO_2 residual	SiO_2 removed (%)	TDS	Reference
Silica seeds	418	180	57	24,153	Setiawan et al. (2019)
Ca(OH)$_2$	400	60	85	5093	Badruk and Matsunaga (2001)
NaOH	600	210	65	15,455	Gallup et al. (2003)
Zn	140	27	81	2830	Zeng et al. (2007)
Mg	450	200	56	n.d.	Lin et al. (2003)
Al	532	100	81	1688	Yokoyama et al. (2002)
Fe	240	84	65	4752	Renew and Hansen (2017)
Cu	600	440	27	15,455	Gallup et al. (2003)

n.d. not determined

5. Conclusions

Within this study, the removal of silica out of thermal brines was investigated. The aim was to minimize the risk of silica scaling which extends the use of geothermal brines as a new source for raw materials. Effective silica removal is achieved via formation of C-S-H phases. The precipitation occurs within minutes and the residual silica concentration remains significantly below the saturation concentration of SiO_2. The reduction below the saturation concentration is reached in under 5 minutes and after 30 minutes after addition of the precipitation agent, the silica removal process is almost completed. For integration of a silica removal processing unit in geothermal power plants fast reaction kinetics are advantageous since it allows a plant design with short hydraulic residence times and as a consequence lower investment costs and smaller space requirement. The developed removal process depends on two major factors that need to be adapted to induce an effective and fast precipitation process:

1) The increase of the pH-value > 10 favors the formation of C-S-H phases. The mechanism is hereby independent of the additives and trace elements.
2) Molar Ca/Si ratios > 1.25 lead to an effective removal of silica.

Further optimizations of the molar Ca/Si ratio need to be performed, to yield maximal silica removal and simultaneously minimal residual calcium concentrations to prevent latter stage calcite scaling. However, the experiments have shown that the silica removal process by formation of C-S-H phases is element-specific. The concentration of Li, as a raw material of current economic interest, remains constant in solution. Additional experiments performed with complex, natural brine confirm the element-specific removal process, which mechanism is also not disturbed by the presence of additional elements in the solution. In general, monovalent ions (Li, Rb, Cs) are not affected by the removal mechanism, while higher valent ions can be incorporated in the precipitates, which is confirmed by ICP-MS analysis of the precipitates. However, the incorporation of trace elements only accounts to a lesser amount (<0.25 %). The precipitates show elevated incorporation of Mg that is quantitatively removed from the solution. Mg, having the same valence as Ca, is presumably forming M-S-H-phases; in analogy with the C-S-H-phases. Therefore, it is likely that sufficient high molar Mg/Si ratios can also lead to effective removal of both Si and Mg.

These findings demonstrate that in silica-rich brines the removal of silica by the formation of C/M-S-H-phases is suitable for brine mining purposes. By reducing the SiO_2 concentration, the risk of silica scaling during further treatment processes is negligible. This is a first important step towards integrating mineral extraction in geothermal systems worldwide and thus enabling local raw material production in Germany again.

Acknowledgements

CRediT authorship contribution statement

Laura Spitzmüller: Methodology, Investigation, Conceptualization, writing – original draft, Formal analysis, Visualization. **Valentin Goldberg:** Methodology, Writing – review & editing. **Sebastian Held:** Conceptualization, Methodology, Resources, Writing – review & editing, Supervision, Project administration, funding acquisition. **Jens C. Grimmer:** Conceptualization, Writing – original draft, review & editing. **Daniel Winter:** Resources, writing – review & editing. **Milena Genovese:** Investigation. **Joachim Koschikowski:** Resources, Supervision. **Thomas Kohl:** Supervision, Writing – review & editing, Funding acquisition.

Conflict of interest

The authors declare there is no conflict of interest.

References

Alexander, G.B., Heston, W.M., Iler, R.K., 1954. The Solubility of Amorphous Silica in Water. The Journal of Physical Chemistry 58 (6), 453–455.

Badruk, M., Matsunaga, I., 2001. Experimental results of silica removal from simulated solutions of geothermal brine of Kizildere field, Turkey. Geothermics 30 (5), 561–570.

Borrmann, T., Johnston, J.H., 2017. Transforming Silica into Silicate - Pilot Scale Removal of Problematic Silica from Geothermal Brine. GRC Transactions 41.

Borrmann, T., Johnston, J.H., McBrearty, R., 2009. Nano-structured Calcium Silicate - A solution to the Formation of Silica Scale in Geothermal Water. Transactions - Geothermal Resources Council.

Bourcier, W.L., Lin, M., Nix, G., 2005. Recovery of Minerals and Metals from Geothermal Fluids.

Bourcier, W.L., Martin, S., Viani, B., Bruton, C., 2001. Developing a Process for Commercial Silica Production from Geothermal Brines. Geothermal Resources Council.

Bourcier, W.L., Ralph, W., Johnson, M., Bruton, C., Gutierrez, P., 2006. Silica Extraction at the Mammoth Lakes Geothermal Site. Geothermal Resources Council.

Bremere, I., Kennedy, M., Mhyio, S., Jaljuli, A., Witkamp, G.-J., Schippers, J., 2000. Prevention of silica scale in membrane systems: removal of monomer and polymer silica. Desalination 132 (1-3), 89–100.

Cairns, M.J., Borrmann, T., Höll, W.H., Johnston, J.H., 2006. A study of the uptake of copper ions by nanostructured calcium silicate. Microporous and Mesoporous Materials 95 (1-3), 126–134.

Eikenberg, J., 1990. On the Problem of Silica Solubility at High pH. Paul Scherer Institut.

Ellis, A.J., Mahon, W.A.J., 1977. Chemistry and geothermal systems. Academic Press, New York, 392 pp.

Finster, M., Clark, C., Schroeder, J., Martino, L., 2015. Geothermal produced fluids: Characteristics, treatment technologies, and management options. Renewable and Sustainable Energy Reviews 50, 952–966.

Fournier, R.O., Rowe, J.J., 1966. Estimation of Underground Temperatures from the Silica Content of Water from Hot Springs and Wet-Steam Wells. American Journal of Science 264, 685–697.

Gallup, D.L., 2002. Investigations of organic inhibitors for silica scale control in geothermal brines. Geothermics 31 (4), 415–430.

Gallup, D.L., 2011. pH Modification Scale Control Technology. Proceedings International Workshop on Mineral Scaling, 39–46.

Gallup, D.L., Barcelon, E., 2005. Investigations of organic inhibitors for silica scale control from geothermal brines–II. Geothermics 34 (6), 756–771.

Gallup, D.L., Sugiaman, F., Capuno, V., Manceau, A., 2003. Laboratory investigation of silica removal from geothermal brines to control silica scaling and produce usable silicates. Applied Geochemistry 18 (10), 1597–1612.

Giggenbach, W., 1978. The isotopic composition of waters from the El Tatio geothermal field, Northern Chile. Geochimica et Cosmochimica Acta 42, 979–988.

Greenberg, S.A., 1954. Calcium Silicate Hydrate (I). J. Phys. Chem. 58 (4), 362–367.

Greenberg, S.A., 1956. The Chemisorption of Calcium Hydroxide by Silica. Journal of Physical Chemistry 60 (3), 325–330.

Grimmer, J.C., Ritter, J.R.R., Eisbacher, G.H., Fielitz, W., 2017. The Late Variscan control on the location and asymmetry of the Upper Rhine Graben. Int J Earth Sci (Geol Rundsch) 106 (3), 827–853.

Gunnarsson, I., Arnórsson, S., 2005. Treatment of Geothermal Waste Water to Prevent Silica Scaling. Proceedings World Geothermal Congress.

Henley, R.W., 1983. pH and Silica Scaling Control in Geothermal Field Development. Geothermics 12 (4), 307–321.

Iler, R.K., 1975. Coagulation of colloidal silica by calcium ions, mechanism, and effect of particle size. Journal of Colloid and Interface Science 53 (3), 476–488.

Iler, R.K., 1979. The chemistry of silica: Solubility, polymerization, colloid and surface properties, and biochemistry. Wiley, New York, NY, 866 pp.

Johnston, J.H., Borrmann, T., Schweig, M., Cairns, M.J., 2019. Developments in the Nanostructured Calcium Silicate Technology for Preventing Silica Deposition and Opening New Business Opportunities. GRC Transactions 43.

Kato, K., Ueda, A., Mogi, K., Nakazawa, H., Shimizu, K., 2003. Silica recovery from Sumikawa and Ohnuma geothermal brines (Japan) by addition of CaO and cationic precipitants in a newly developed seed circulation device. Geothermics 32 (3), 239–273.

Kesler, S.E., Gruber, P.W., Medina, P.A., Keoleian, G.A., Everson, M.P., Wallington, T.J., 2012. Global lithium resources: Relative importance of pegmatite, brine and other deposits. Ore Geology Reviews 48, 55–69.

Kiyota, Y., Uchiyama, N., 2011. Silica scale prevention effects of brine pH modification at Hatchobaru power station, Japan. Proceedings International Workshop on Mineral Scaling.

Lee, C.-G., Alvarez, P.J.J., Kim, H.-G., Jeong, S., Lee, S., Lee, K.B., Lee, S.-H., Choi, J.-W., 2018. Phosphorous recovery from sewage sludge using calcium silicate hydrates. Chemosphere 193, 1087–1093.

Lin, M.S., Premuzic, E.T., Dong, B., Zhou, W.M., Johnson, S.D., 2003. Recent Advances in the Development and Commercialisation of Geothermal Silica Products. Geothermal Resources Council Transactions 27, 547–550.

Lin, M.S., Premuzic, E.T., Zhou, W.M., Dong, B., DeRocher, T., Johnson, S.D., 2002. Silica Recovery: A Promising Option to Reduce Geothermal Power Plant Production Costs. Geothermal Resources Council Transactions 26, 149–152.

Maimoni, A., 1982. Minerals Recovery from Salton Sea Geothermal Brines: A Literature Review and proposed Cementation Process. Geothermics 11 (4), 239–258.

Maraghechi, H., Rajabipour, F., Pantano, C.G., Burgos, W.D., 2016. Effect of calcium on dissolution and precipitation reactions of amorphous silica at high alkalinity. Cement and Concrete Research 87, 1–13.

Mathieux, F., Ardente, F., Bobba, S., Nuss, P., Blengini, G.A., Alves, P., Blagoeva, D., Torres de Matos, C., Wittmer, D., Pavel, C., Šolar, S.V., 2017. Critical raw materials and the circular economy: JRC science for policy report : background report. EUR (Luxembourg. Online) 28832. Publications Office of the European Union, Luxembourg, 1 online resource.

Milne, N.A., O'Reilly, T., Sanciolo, P., Ostarcevic, E., Beighton, M., Taylor, K., Mullett, M., Tarquin, A.J., Gray, S.R., 2014. Chemistry of silica scale mitigation for RO desalination with particular reference to remote operations. Water research 65, 107–133.

Morita, M., Goto, Y., Motoda, S., Fujino, T., 2017. Thermodynamic Analysis of Silica-Based Scale Precipitation Induced by Magnesium Ion. Journal of the Geothermal Research Society of Japan 39 (4), 191–201.

Mroczek, E., Climo, M., Li, Y., Evans, D., Carey, B., Gao, W., 2015. From Waste to Wealth: Mineral Extraction from Geothermal Brines. World Geothermal Congress.

Neofotistou, E., Demadis, K.D., 2004. Silica scale inhibition by polyaminoamide STARBURST® dendrimers. Colloids and Surfaces A: Physicochemical and Engineering Aspects 242 (1-3), 213–216.

Neupane, G., Wendt, D.S., 2017. Assessment of Mineral Resources in Geothermal Brines in the US. Proceedings 42nd Workshop on Geothermal Reservoir Engineering.

Putera, A.D.P., Wiranda, A., Mergiana, S., Perdana, I., Olvianas, M., 2018. Assessing silica precipitation using calcium hydroxide addition on Dieng's geothermal brine. IOP Conference Series: Earth and Environmental Science 200.

Renew, J., Hansen, T., 2017. Geothermal Thermoelectric Generation (G-TEG) with Integrated Temperature Driven Membrane Distillation and Novel Manganese Oxide for Lithium Extraction.

Rothbaum, H.P., Anderton, B.H., 1975. Removal of Silica and Arsenic from Geothermal Discharge Waters by Precipitation of Useful Calcium Silicates. Second United Nations Symposium on the development and use of geothermal resources, 1417–1425.

Rothbaum, H.P., Anderton, B.H., Harrison, R.F., Rohde, A.G., Slatter, A., 1979. Effect of silica polymerisation and pH on geothermal scaling. Geothermics 8 (1), 1–20.

Ryu, T., Haldorai, Y., Rengaraj, A., Shin, J., Hong, H.-J., Lee, G.-W., Han, Y.-K., Huh, Y.S., Chung, K.-S., 2016. Recovery of Lithium Ions from Seawater Using a Continuous Flow Adsorption Column Packed with Granulated Chitosan–Lithium Manganese Oxide. Ind. Eng. Chem. Res. 55 (26), 7218–7225.

Sanjuan, B., Millot, R., Innocent, C., Dezayes, C., Scheiber, J., Brach, M., 2016. Major geochemical characteristics of geothermal brines from the Upper Rhine Graben granitic basement with constraints on temperature and circulation. Chemical Geology 428, 27–47.

Schmidt, M., 2017. Rohstoffrisikobewertung - Lithium. DERA Rohstoffinformationen.

Setiawan, F.A., Rahayuningsih, E., Tri, H., Murti, B., Nurpratama, M.I., 2019. Kinetics of silica precipitation in geothermal brine with seeds addition: minimizing silica scaling in a cold re-injection system. Geothermal Energy 7 (1).

Sigfusson, B., Gunnarsson, I., 2011. Scaling Prevention Experiments in the Hellisheiði Power Plant, Iceland. Proceedings Thirty-Sixth Workshop on Geothermal Reservoir Engineering.

Stober, I., 2002. Geologie und Geschichte der Mineral- und Thermalquellen im Schwarzwald. Ber. Naturf. Ges. Freiburg i. Br. 92 (2), 29–52.

Sugita, H., Kato, K., Ueda, A., Matsunaga, I., Sakurai, Y., Yasuda, K., Bando, Y., Nakamura, M., 1999. Field Tests on Silica Removal from Geothermal Brines in Sumikawa and Onuma Geothermal Areas. Journal of chemical engineering of Japan 32 (5), 696–700.

Sugita, H., Matsunaga, I., Yamaguchi, T., 2000. Silica Scale Prevention Method using Seed Made from Geothermal Brine. Proceedings World Geothermal Congress.

Sugita, H., Matsunaga, I., Yamaguchi, T., Kato, K., Ueda, A., 2003. Silica removal performance of seed from geothermal fluids. Geothermics 32 (2), 171–185.

Tassi, F., Aguilera, F., Darrah, T., Vaselli, O., Capaccioni, B., Poreda, R.J., Delgado Huertas, A., 2010. Fluid geochemistry of hydrothermal systems in the Arica-Parinacota, Tarapacá and Antofagasta regions (northern Chile). Journal of Volcanology and Geothermal Research 192 (1-2), 1–15.

Vitolo, S., Cialdella, M.L., 1994. Silica separation from reinjection brines at Monte Amiata geothermal plants, Italy. Geothermics 23 (3), 257–266.

Yokoyama, T., Takahashi, Y., Yamanaka, C., Tarutani, T., 1989. Effect of aluminium on the polymerization silicic acid in aqueous solution and the deposition of silica of silica. Geothermics 18 (1-2), 321–326.

Yokoyama, T., Ueda, A., Kato, K., Mogi, K., Matsuo, S., 2002. A study of the alumina-silica gel adsorbent for the removal of silicic acid from geothermal water: increase in adsorption capacity of the adsorbent due to formation of amorphous aluminosilicate by adsorption of silicic acid. Journal of Colloid and Interface Science 252 (1), 1–5.

Zeng, Y., Yang, C., Pu, W., Zhang, X., 2007. Removal of silica from heavy oil wastewater to be reused in a boiler by combining magnesium and zinc compounds with coagulation. Desalination 216 (1-3), 147–159.

Appendix

Table 4. Overview of the experimental parameters and ICP-OES results of the experiments with synthetic produced water (mg/L, unless otherwise noted). The names of the experiments are used to differ between different experimental parameters. The reference is linked to the Figures in which the results are shown. For further explanation, the reader is referred to Chapter 2.

Experiment number	Sample ID	Method	Reaction Time (min)	Temperature (°C)	pH (-)	Ca/Si (molar)	SiO_2	Li	Na	Ca	K	Reference
1	Ex. 1.0	Si-Seeds	0				317,65	32.19	3818.89	3.65	536.10	Fig. 2, Fig. 3
1	Ex. 1.1	Si-Seeds	5				303.06	30.34	3641.59	5.02	516.49	Fig. 2, Fig. 3
1	Ex. 1.2	Si-Seeds	10				290.76	30.01	3559.11	4.04	499.45	Fig. 2, Fig. 3
1	Ex. 1.3	Si-Seeds	20				295.82	30.25	3627.75	4.09	513.11	Fig. 2, Fig. 3
1	Ex. 1.4	Si-Seeds	30				286.02	29.78	3563.84	4.85	506.63	Fig. 2, Fig. 3
1	Ex. 1.5	Si-Seeds	60				268.30	27.15	3227.38	5.45	452.28	Fig. 2, Fig. 3
1	Ex. 1.6	Si-Seeds	90				276.13	27.62	3382.34	4.47	471.02	Fig. 2, Fig. 3
1	Ex. 1.7	Si-Seeds	120				258.63	25.93	3139.87	5.05	444.38	Fig. 2, Fig. 3, Fig. 8, Fig. 11
2	Ex. 2.0	$CaCl_2$	0	69.9	6.7	0.95	321.65	30.11	3693.88	205.04	537.03	Fig. 2
2	Ex. 2.1	$CaCl_2$	15	68.5	6.86	2	329.88	30.83	3768.89	515.36	555.93	Fig. 2
2	Ex. 2.2	$CaCl_2$	30	68.3	7.15	2	332.11	31.48	3832.11	521.70	567.77	Fig. 2
2	Ex. 2.3	$CaCl_2$	60	69.3	6.7	2	331.21	31.04	3821.46	520.78	563.69	Fig. 2
2	Ex. 2.4	$CaCl_2$	120	70	6.45	2	329.38	30.29	3722.04	501.82	561.46	Fig. 2
3	Ex. 3	$CaCl_2$ + NaOH	120	69.7	7.96	2	288.91	26.49	3277.49	369.81	491.92	Fig. 9
4	Ex. 4	$CaCl_2$ + NaOH	120	69.5	8.97	2	330.28	30.74	3822.48	429.27	554.70	Fig. 9
5	Ex. 5	$CaCl_2$ + NaOH	120	70.1	9.48	2	304.11	28.35	3619.62	398.01	510.76	Fig. 9
6	Ex. 6	$CaCl_2$ + NaOH	120	70.3	10.02	2	262.43	28.99	3771.95	385.48	527.45	Fig. 9
7	Ex. 7	$CaCl_2$ + NaOH	120	70.4	10.47	2	42.28	25.76	3389.37	226.72	460.91	Fig. 8, Fig. 9
8	Ex. 8	$CaCl_2$ + NaOH	120	69.9	10.34	0.5	201.95	34.0	3974	53	567	Fig. 8
9	Ex. 9	$CaCl_2$ + NaOH	120	69.5	10.46	0.8	80.65	34	4378	96	580	Fig. 8
10	Ex. 10	$CaCl_2$ + NaOH	60	68.7	10.52	0.95	90.13	96.19		63.15		Fig. 8

No.	Name	Reagent	Reaction Time (min)	Temperature (°C)	pH (-)							Figure
11	Ex. 11	CaCl$_2$ + NaOH	60	68.9	10.57	1.25	36.17	99.79		89.69		Fig. 8
12	Ex. 12	CaCl$_2$ + NaOH	60	65.8	10.53	1.5	23	95.75		198.17		Fig. 8
13	Ex. 13	CaCl$_2$ + NaOH	60	67.9	10.52	1.75	20.91	95.62		252.92		Fig. 8
14	Ex. 14	CaCl$_2$ + NaOH	60	65.7	10.52	2	26.4	111.73		340.63		Fig. 8
15	Ex. 15	CaCl$_2$ + NaOH	60	67.9	10.49	3	66.11	94.01		658.69		Fig. 8
16	Ex. 16.0	Ca(OH)$_2$	0	69.5	6.7	0	314.26	29,48	3787,95	185.71	551.78	Fig. 2,Fig. 3, Fig. 8
16	Ex. 16.1	Ca(OH)$_2$	5	68.9	10.46	2.36	111.90	31.05	3943.58	307.01	563.70	Fig. 3, Fig. 8
16	Ex. 16.2	Ca(OH)$_2$	10	67.8	10.36	2.36	91.81	31.08	3975.59	315.02	565.30	Fig. 3, Fig. 8
16	Ex. 16.3	Ca(OH)$_2$	15	68.1	10.45	2.36	71.87	31.31	3995.13	329.73	575.49	Fig. 3, Fig. 8
16	Ex. 16.4	Ca(OH)$_2$	20	68	10.44	2.36	53.77	31.57	4008.48	324.68	575.48	Fig. 3, Fig. 8
16	Ex. 16.5	Ca(OH)$_2$	30	67.7	10.42	2.36	32.10	31.42	4001.58	326.10	572.31	Fig. 3, Fig. 8
16	Ex. 16.6	Ca(OH)$_2$	60	68.8	10.47	2.36	21.93	31.00	3971.89	316.99	572.35	Fig. 3, Fig. 8
16	Ex. 16.7	Ca(OH)$_2$	90	69.4	10.5	2.36	16.96	30.44	3861.12	308.19	552.18	Fig. 3, Fig. 8
16	Ex. 16.8	Ca(OH)$_2$	120	69.2	10.59	2.36	14.75	30.45	3876.67	309.82	560.50	Fig. 3, Fig. 4, Fig. 8, Fig. 9 Fig. 11
17	Ex. 17	Ca(OH)$_2$	120	70.8	8.3	1	318.27	32.26	3997.84	229.33	557.74	Fig. 9
18	Ex. 18	Ca(OH)$_2$	120	70.3	9.15	1.25	283.41	30.13	3771.99	257.48	530.20	Fig. 9
19	Ex. 19	Ca(OH)$_2$	120	71.2	9.7	1.5	275.16	31.10	3997.25	318.17	560.53	Fig. 9
20	Ex. 20	Ca(OH)$_2$	120	71.4	10.02	1.75	154.79	31.44	3968.33	312.97	552.68	Fig. 9
21	Ex. 21	Ca(OH)$_2$	120	71.6	10.12	2	29.43	31.51	4006.27	298.07	562.08	Fig. 9
22	Ex. 22	NaOH	120	69.6	10.5	0	329.05	30.54	4098.99	1	562.33	Fig. 8
23	Ex. 23.0	NaOH	0			0.95	327.81	30.12	3860.50	2.35	540.30	Fig. 2
23	Ex. 23.1	NaOH	120	69.5	10.46	0.95	60.11	29.53	4039.48	66.57	543.04	Fig. 2, Fig. 9, Fig. 11

Table 5. ICP-OES results (mg/L, unless otherwise noted) and experimental parameters of the precipitation experiments using the Baden-Baden brine (Fettquelle "FQ"). For further explanation, the reader is referred to Chapter 2.

Name	Reaction Time (min)	Temperature (°C)	pH (-)	SiO$_2$	Li	Na	Ca	K	Mg	Rb	Sr	As	Ba
FQ		61		146.99	9.38	92.48	135.44	86.52	4.08	1.10	3.03	0.28	0.16
Bad 1	0	69.8	8.11	287.42	92.90	1717.68	168.48	160.14	7.55	2.59	6.39	0.44	0.32
Bad 1	2	71.4	9.44	215.66	101.28	2051.29	186.15	174.13	0.21	2.49	5.75	0.21	0.28

Bad 1	15	72.1	10.85	45.06	100.38	2051.53	168.78	176.31	0.23	2.43	5.57	0.19	0.25
Bad 1	30	69.4	10.93	24.96	99.61	2033.93	173.35	175.02	<0.1	2.26	5.41	0.16	0.25
Bad 1	60	70.2	10.87	17.17	100.25	2048.81	166.77	175.86	<0.1	2.21	5.39	0.09	0.25
Bad 1	120	69.9	10.89	16.43	101.13	2072.44	159.52	177.36	<0.1	2.32	5.33	0.11	0.25
Bad 2	0	70	7.9	288.84	95.69	1845.15	175.80	172.01	7.83				
Bad 2	6	70.1	11.34	36.60	97.49	2129.40	244.03	176.61	<0.1				
Bad 2	16	70.2	11.44	10.40	97.09	2152.00	267.87	208.43	<0.1				
Bad 2	40	70.2	11.39	6.61	90.29	2101.62	221.28	168.58	<0.1				
Bad 2	60	69.6	11.4	12.98	95.00	2120.99	256.46	205.13	<0.1				
Bad 2	126	69.4	11.26	6.92	93.30	2060.75	235.42	201.86	<0.1				
Bad 3	0	70.9	7.97	295.42	96.47	1884.04	178.77	175.06	7.97				
Bad 3	5	71.2	11.36	18.15	97.03	224.40	194.56	177.82	<0.1				
Bad 3	15	69.5	11.41	9.20	94.45	2198.45	208.42	176.69	<0.1				
Bad 3	30	68.8	11.38	12.88	94.16	2086.15	258.39	202.46	<0.1				
Bad 3	59	67.9	11.37	5.83	96.51	2227.50	229.45	178.90	<0.1				
Bad 3	114	73.2	11.32	6.89	98.02	2301.61	207.15	186.91	<0.1				

Table 6. ICP-MS results of the precipitates. For FQ the water analysis of Sanjuan et al. (2016) is used. (ppm, unless otherwise noted).

Component	FQ (µg/L)[1]	Bad-1 Precipitate	Bad-2 Precipitate	Bad-3 Precipitate
Li[2]	100,000	90.7	28.4	17.4
B	3600	126	118	113
Al	10.78	102	163	139
Ti	n.d.	9.13	16.4	12.8
V	n.d.	0.27	0.74	0.82
Cr	<1	1.32	1.51	0.82
Mn	17.62	431	172	601
Fe	60	200	234	304
Co	<0.5	0.06	0.1	0.08
Ni	<1	1.16	1.6	1.63
Cu[3]	<1	224	1.99	5.5
Zn	<5	136.2	12.1	11.1
As	352	344	335	329

Rb	2880	12.4	2.83	2
Sr	7000	613	450	555
Y	n.d.	1.04	1.86	1.44
Mo	n.d.	0.03	0.01	0.02
Ag	<0.1	1.97	6.02	6.31
Cd	<0.1	0.05	0.07	0.06
Sb	n.d.	1.24	3.01	1.84
Cs[4]	10,000	74	15.8	9.82
Ba	238	87.3	78.8	76.6
Tl	n.d.	3.03	5.05	4.2
Pb	<0.5	0.49	0.52	0.89
U	0.66	0.15	0.18	0.2

[1] Twice the concentrations obtained by Sanjuan et al. (2016)

[2] Addition of 84 mg/L Li by LiCl

[3] Addition of 0.5 mg/L Cu by $CuSO_4$ in Bad-1

[4] Addition of 10 mg/L Cs by CsCl